Electronic Structure of Mo(VI) Alkylidene Complexes and an Examination of Reactive Intermediates Using the SCF-Xα-SW Method

Harold H. Fox, Mark H. Schofield, and Richard R. Schrock*

Department of Chemistry, Massachusetts Institute of Technology, Room 6-331, Cambridge, Massachusetts 02193

Received January 25, 1994®

SCF-Xα-SW calculations were carried out on Mo(VI) imido alkylidene complexes, Mo(NH)$(CH_2)(OH)_2$ (1), Mo(NH)$(CH_2)(OCH_3)_2$ (2), a complex in which the alkylidene ligand has been rotated 90° (3), and the molybdacyclobutane complex, Mo(NH)$(CH_2CH_2CH_2)(OH)_2$ (4). In the basic model (1) the HOMO is the relatively nonpolar Mo–C π-bond; the contributions by the C 2p and the Mo 4d atomic orbitals are approximately equal. An agostic interaction involving the C–H_{anti} bond in the methylene ligand in 1 can be identified. The alkoxide oxygen 2p orbitals contribute to a significant extent to most molecular orbitals in 1, and consequently the alkoxides strongly influence the reactivity of the complexes. The LUMO in 1 is the M–N π-antibonding orbital in the alkylidene plane, which is largely metal-centered on the COO face of the pseudotetrahedral complex. The electronic structure of 2 is roughly the same as 1. Alkylidene rotation in 1 is explored and the evolution of molecular orbitals during this process is discussed. Bending of the imido proton toward the alkylidene ligand is an important stabilizing feature in the "rotated" alkylidene complex, lowering the activation energy for rotation by approximately 50%. Calculations suggest that 4 can form readily when ethylene approaches the COO face of 3.

Introduction

Four-coordinate "d^0" imido alkylidene complexes of the type Mo(NR)(CHR')$(OR'')_2$, which are catalysts for the metathesis of acyclic and cyclic olefins,[1-10] can now be synthesized with significant variation in the nature of the OR'' and (to some extent) the NR ligands in four steps starting from $[NH_4]_2[Mo_2O_7]$.[11-13] An important feature of catalysts of this type is the ability to control their activity by varying the steric and electronic nature of the OR'' ligands; in general the more electron-withdrawing alkoxide ligands (e.g., fluorinated *tert*-butoxides) give rise to more active catalysts.[9,10] Recently it has been shown that alkylidene rotamers (syn and anti) are present in such complexes, that syn and anti rotamers interconvert in *tert*-butoxide complexes approximately 6 orders of magnitude faster than in hexafluoro *tert*-butoxide complexes, and that the reactivities of syn and anti rotamers can differ dramatically.[5,9] Preliminary results suggest that at least some all trans polymers produced via ring-opening metathesis polymerization arise via anti intermediates, while cis polymers arise via syn intermediates,[9] and that catalysts that contain chiral diolate ligands lead to tactic polymers via enantiomorphic site control.[6]

The electronic structure of "d^0" alkylidene complexes has been examined in a number of theoretical studies.[14-22] In early studies the complexes that were chosen for the calculation did not model a real catalyst, primarily because well-characterized species had not yet been prepared. The majority of the theoretical studies have dealt primarily with structure,[15,17,20-22] while others have been concerned more with the mechanism of olefin metathesis.[14,16,18,19] Two relatively recent and thorough studies concentrated on imido alkylidene complexes,[14,16] in part because of the relatively large amount of experimental data available for such species. Cundari and Gordon explored the electronic structure of a variety of alkylidene complexes of the type M(NH)$(CH_2)(OH)_2$ (M = Mo, W) and Re(CH)$(CH_2)(OH)_2$ at the ab initio level.[16] The π molecular orbitals were presented for the alkylidene and the imido (or alkylidyne) ligands, and the polarity of the metal–carbon double bond was discussed in detail. Structures were optimized at the Hartree–Fock level and found to agree well with experi-

• Abstract published in *Advance ACS Abstracts*, June 1, 1994.

(1) (a) Bazan, G.; Khosravi, E.; Schrock, R. R.; Feast, W. J.; Gibson, V. C.; O'Regan, M. B.; Thomas, J. K.; Davis, W. M. *J. Am. Chem. Soc.* **1990**, *112*, 8378. (b) Feast, W. J.; Gibson, V. C.; Marshal, E. L. *J. Chem. Soc., Chem. Commun.* **1992**, 1157.

(2) Fox, H. H.; Schrock, R. R. *Organometallics* **1992**, *11*, 2763.

(3) (a) Fu, G. C.; Grubbs, R. H. *J. Am. Chem. Soc.* **1992**, *114*, 5426. (b) Fu, G. C.; Grubbs, R. H. *J. Am. Chem. Soc.* **1992**, *114*, 7324.

(4) (a) Smith, D. W., Jr.; Wagener, K. B. *Macromolecules* **1993**, *26*, 1633. (b) Wagener, K. B.; Boncella, J. M.; Nel, J. G. *Macromolecules* **1991**, *24*, 2649.

(5) Oskam, J. H.; Schrock, R. R. *J. Am. Chem. Soc.* **1992**, *114*, 7588.

(6) McConville, D. H.; Wolf, J. R.; Schrock, R. R. *J. Am. Chem. Soc.* **1993**, *115*, 4413.

(7) Fox, H. H.; Lee, J.-K.; Park, L. Y.; Schrock, R. R. *Organometallics* **1993**, *12*, 759.

(8) Crowe, W. E.; Zhang, Z. J. *J. Am. Chem. Soc.* **1993**, *115*, 10998.

(9) Oskam, J. H.; Schrock, R. R. *J. Am. Chem. Soc.* **1993**, *115*, 11831.

(10) Fox, H. H.; Schrock, R. R.; O'Dell, R. *Organometallics* **1994**, *13*, 635.

(11) Schrock, R. R.; Murdzek, J. S.; Bazan, G. C.; Robbins, J.; DiMare, M.; O'Regan, M. *J. Am. Chem. Soc.* **1990**, *112*, 3875.

(12) Oskam, J. H.; Fox, H. H.; Yap, K. B.; McConville, D. H.; O'Dell, R.; Lichtenstein, B. J.; Schrock, R. R. *J. Organomet. Chem.* **1993**, *459*, 185.

(13) Fox, H. H.; Yap, K. B.; Robbins, J.; Cai, S.; Schrock, R. R. *Inorg. Chem.* **1992**, *31*, 2287.

(14) Folga, E.; Ziegler, T. *Organometallics* **1993**, *12*, 325.

(15) Cundari, T. R.; Gordon, M. S. *J. Am. Chem. Soc.* **1992**, *114*, 539.

(16) Cundari, T. R.; Gordon, M. S. *Organometallics* **1992**, *11*, 55.

(17) Sodupe, M.; Lluch, J. M.; Oliva, A.; Bertrán, J. *Organometallics* **1989**, *8*, 1837.

(18) Volatron, F.; Eisenstein, O. *J. Am. Chem. Soc.* **1986**, *108*, 2173.

(19) Upton, T. H.; Rappé, A. K. *J. Am. Chem. Soc.* **1985**, *107*, 1206.

(20) Francl, M. M.; Pietro, W. J.; Hout Jr., R. F.; Hehre, W. J. *Organometallics* **1983**, *2*, 281.

(21) Rappé, A. K.; Goddard W. A., III. *J. Am. Chem. Soc.* **1982**, *104*, 297.

(22) Goddard, R. J.; Hoffmann, R.; Jemmis, E. D. *J. Am. Chem. Soc.* **1980**, *102*, 7667.

0276-7333/94/2313-2804$04.50/0

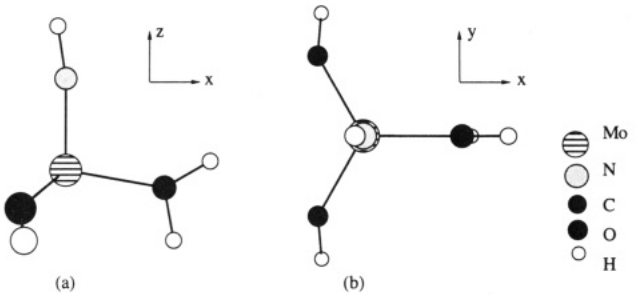

Figure 1. Representation of $Mo(NH)(CH_2)(OH)_2$ (1), used as a model in SCF–Xα–SW calculations in (a) the *xz* plane and (b) the *xy* plane.

mentally determined structures. The authors also examined the consequence of rotating the alkylidene ligand and altering the electronic nature of the alkylidene ligand. Folga and Ziegler explored the electronic nature of $Mo(NH)(CH_2)(OH)_2$ and the mechanism of metallacycle formation employing the HFS-LCAO method (Hartree–Fock–Slater linear combinations of atomic orbitals).[14] Concentrating on pathways for forming square pyramidal and trigonal bipyramidal metallacyclobutane complexes of known structure, they found that metallacycles form via olefin coordination to the metal followed by C–C π-bond breaking with concomitant C–C bond formation and rehybridization of sp^2 carbons to sp^3 carbons. In this study it apparently was assumed that the metallacyclobutane complexes that have been structurally characterized lie on the metathesis reaction pathway.

Calculations employing the self-consistent field-Xα-scattered wave (SCF–Xα–SW)[23,24] method are well-suited to transition metal complexes.[24] For example, we have employed the SCF–Xα–SW method recently to explore the electronic structure of tungsten,[25] rhenium,[25] and osmium[26] imido complexes. In this paper we use the SCF–Xα–SW method to explore molybdenum imido alkylidene complexes. We are particularly interested in the effect of varying the Mo–N–H and the Mo–C–H angles and the orbital evolution during alkylidene ligand rotation, two features that were overlooked in most other studies. We are also interested in an alternative method of forming the metallacyclobutane intermediate that involves a complex in which the alkylidene ligand is rotated by 90° from the favored conformation. These studies are complementary to the ab initio studies of Cundari and Gordon[16] and Folga and Ziegler.[14]

Results

SCF–Xα–SW Analysis of Ground State Structures. $Mo(NH)(CH_2)(OH)_2$ (1; Figure 1), a model for metathetically active Mo imido alkylidene complexes of the type $Mo(NR)(CHR')(OR'')_2$, was employed for most calculations. The Mo–N vector is defined as the *z* axis and the C–Mo–N plane is defined as the *xz* plane (Figure 1). Bond lengths and bond angles were chosen on the basis of those found in the X-ray structure of the first insertion product of the reaction between 7-isopropylidene-2,3-dicarbomethoxynorbornadiene and $Mo(N\text{-}2,6\text{-}i\text{-}Pr_2C_6H_3)(CHCMe_3)(O\text{-}t\text{-}Bu)_2$[1] or in $W(N\text{-}2,6\text{-}i\text{-}Pr_2C_6H_3)(CHCMe_3)(O\text{-}t\text{-}Bu)_2$.[27] Both alkoxide ligands in 1 were oriented in the same manner in order to give 1 idealized C_s symmetry. The CH, NH, and OH bond lengths in 1 were set at 1.0 Å. The methylene protons lie in the N–Mo–C plane, either pointing toward (H_{syn}) or away from (H_{anti}) the nitrogen atom of the imido ligand. The Mo–C–H_{syn} angle was chosen to be 140° and the H–C–H angle was chosen to be 110°. (Mo–C_α–C_β = 140.0 (3)° in the Mo X-ray structure noted above and H–C–H = 112.3 (2)° in the neutron diffraction study of $Ta(\eta^5\text{-}C_5H_5)_2(CH_3)(CH_2)$.[28]) The imido proton was bent slightly away from the *z* axis in the *xz* plane, anti to the alkylidene carbon atom (Mo–N–H = 171°; H–N–Mo–C = 180°). (Mo–N–C = 171.7 (3)° in the Mo X-ray structure noted above.) Bond lengths and angles, dihedral angles, and atomic coordinates for 1 can be found in Tables S1 and S2 in the supplementary material.

The ground state valence molecular orbital energies, occupations, and charge distributions found for 1 are compiled in Table 1. We will focus on the π-bonding and π-antibonding molecular orbitals with carbon and nitrogen character. The HOMO (6a″; Figure 2a) is a Mo–C π-bonding interaction; contributions from the nitrogen 2p (1%) and oxygen 2p (2.5% each) atomic orbitals are minimal. The charge is evenly distributed between Mo and C centers, as found in another study.[16] The Mo–C π-antibonding combination, the 7a″ orbital (Figure 2b), has an energy almost 3.7 eV higher than that of the 6a″ orbital. The 5a″ orbital, which is comprised of the Mo–N π-bond perpendicular to the *xz* plane (Figure 2c) and π-antibonding contributions from the O 2p orbitals (15.5% each), is nearly 1.8 eV lower in energy than the 6a″ orbital, although the molecular orbital is somewhat "nonbonding" (5% metal-based). The 10a′ orbital describes the other Mo–N π-bond parallel to the *xz* plane (Figure 2d). The 4a″ orbital is almost exclusively O-based. The LUMO, the 11a′ orbital, is largely π-antibonding in nature (Figure 2e), metal-based (62%), and oriented so that bases that attack it would approach the metal approximately either on the COO face or the NOO face of the pseudotetrahedron. The 7a″ orbital, which is only ~0.6 eV higher in energy than the 11a′ orbital, would be attacked by bases that approach the metal on one of the equivalent CNO faces of the pseudotetrahedron. If an incoming olefin were to attack the CNO face, a metallacycle could form without rotation of the alkylidene about the Mo–C bond. A metallacycle could result from olefin attack on the COO face, *if* the alkylidene ligand rotates about the Mo–C bond by 90°. Olefin attack on the NOO face (trans to the alkylidene ligand) should not readily lead to formation of a metallacycle.

The oxygen 2p orbitals contribute to most of the valence molecular orbitals in 1 to a significant degree (Table 1). For this reason, it is not surprising that the reactivity of the complexes changes dramatically with changes in the electronic nature of the alkoxide ligand.[9-11] With this in mind, it is useful to examine a more realistic model, $Mo(NH)(CH_2)(OMe)_2$ (2; Figure 3). Bond lengths and angles were chosen as described above for 1 (see Tables S3 and S4 in supplementary material). The methyl protons in

(23) Johnson, K. H. *Adv. Quantum Chem.* **1972**, *7*, 143.
(24) Case, D. *Ann. Rev. Phys. Chem.* **1982**, *33*, 151.
(25) Williams, D. S.; Schofield, M. H.; Schrock, R. R. *Organometallics* **1993**, *12*, 4560.
(26) Schofield, M. H.; Kee, T. P.; Anhaus, J. T.; Schrock, R. R. *Inorg. Chem.* **1991**, *30*, 3595.
(27) Schrock, R. R.; DePue, R. T.; Feldman, J.; Yap, K. B.; Yang, D. C.; Davis, W. M.; Park, L. Y.; DiMare, M.; Schofield, M.; Anhaus, J.; Walborsky, E.; Evitt, E.; Krüger, C.; Betz, P. *Organometallics* **1990**, *9*, 2262.
(28) Takusagawa, F.; Koetzle, T. F.; Sharp, P. R.; Schrock, R. R. *Acta Cryst.* **1988**, *C44*, 439.

Table 1. Energy, Occupancy, and Charge Distribution of the Valence Molecular Orbitals of 1[a]

			charge distribution (%)[b]									
level	energy (eV)	occup[c]	Mo	N	H_{imide}	C	H_{syn}	H_{anti}	O	$H_{hydroxide}$	inter-sphere	outer-sphere	Mo basis functions
14a′	−0.278	0	8	5	0	1	0	0	5	8	36	45	
8a″	−0.434	0	28	1	0	0	0	0	6	1	24	40	p (2) d (98)
13a′	−0.617	0	28	3	1	1	0	0	8	0	36	21	p (11) d (89)
12a′	−1.236	0	9	1	0	0	0	0	3	0	47	38	
7a″	−1.445	0	45	7	0	15	0	0	2	0	24	7	d (100)
11a′	−2.080	0	62	10	0	0	0	1	8	0	16	2	p (1) d (99)
6a″	−5.129	2	33	1	0	29	0	0	5	1	30	2	p (5) d (95)
5a″	−6.939	2	5	42	0	0	0	0	31	0	21	1	
10a′	−7.405	2	11	39	0	3	0	1	26	0	20	1	s (12) p (8) d (80)
4a″	−7.827	2	2	2	0	0	0	0	77	0	19	1	
9a′	−8.059	2	16	7	0	25	2	1	33	0	14	1	s (33) p (23) d (44)
8a′	−8.747	2	16	11	0	3	0	1	49	0	19	0	s (3) p (10) d (87)
3a″	−9.387	2	22	13	0	0	0	0	46	0	19	0	d (100)
7a′	−9.715	2	33	0	0	18	1	2	36	0	10	0	s (2) p (3) d (96)
6a′	−13.033	2	3	1	0	45	20	16	10	3	0	1	
5a′	−13.640	2	13	4	1	13	8	3	53	14	0	1	s (34) p (12) d (54)
2a″	−14.081	2	19	0	0	0	0	0	63	17	0	1	p (15) d (85)
4a′	−14.896	2	34	49	12	0	0	0	4	1	0	0	s (5) p (18) d (77)
3a′	−19.072	2	2	0	0	61	17	19	0	0	0	1	
2a′	−22.017	2	5	72	22	0	0	0	0	0	0	0	
1a″	−24.980	2	4	0	0	0	0	0	82	13	0	0	
1a′	−25.012	2	3	0	0	0	0	0	83	14	0	0	

[a] The coordinate system is shown in Figure 1. Levels above 6a″ are virtual (unoccupied) levels. [b] % of total charge density. [c] Occupancy in electrons.

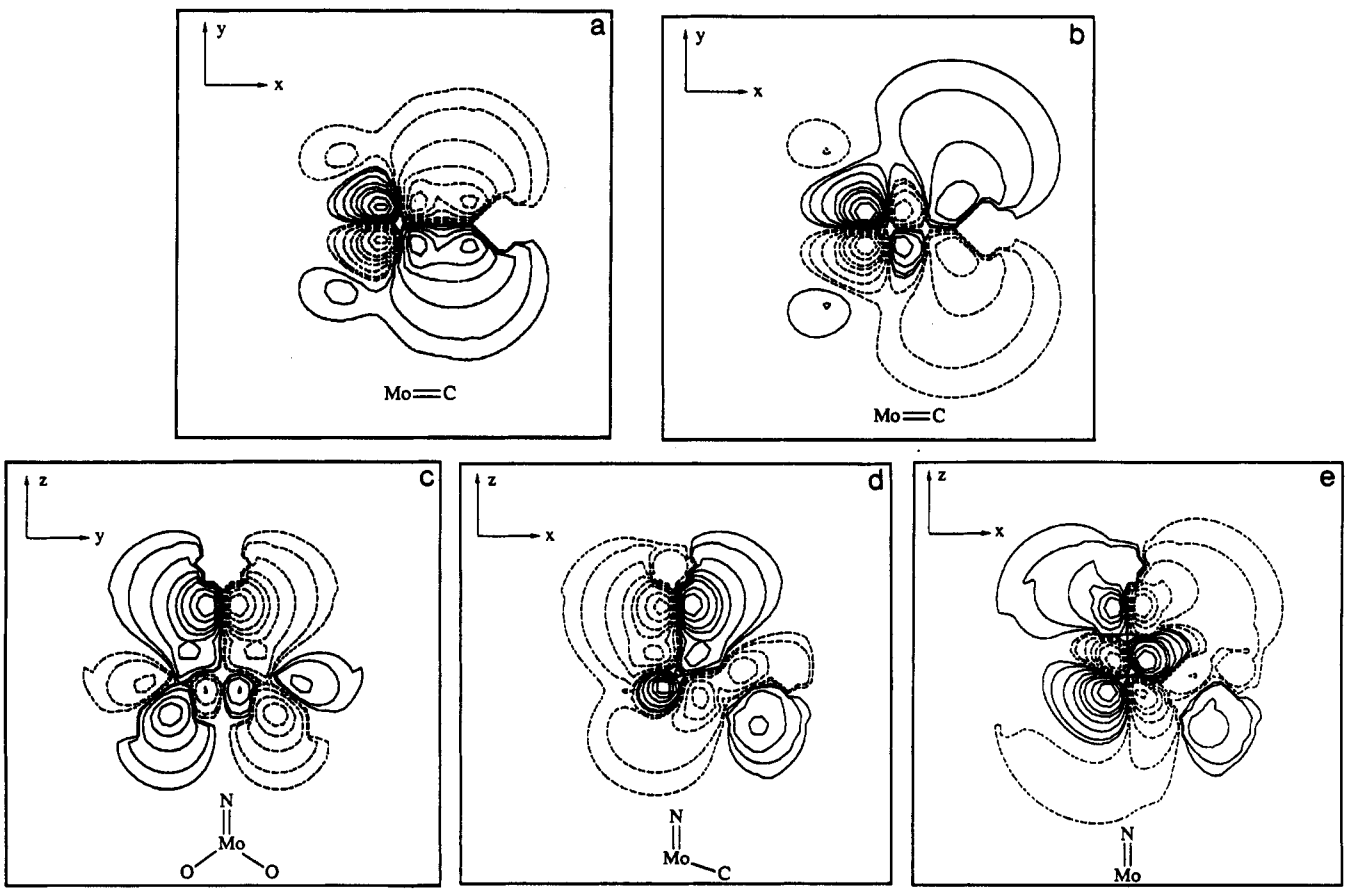

Figure 2. Contour plots showing: (a) the Mo–C π-bonding interaction of the 6a″ orbital (HOMO) in the xy plane; (b) the Mo–C π-antibonding interaction of the 7a″ orbital in the xy plane; (c) the Mo–N π-bonding interaction of the 5a″ orbital in the yz plane; (d) the Mo–N π-bonding interaction of the 10a′ orbital in the xz plane; and (e) the Mo–N π-antibonding interaction of the 11a′ orbital in the xz plane in **1**.

the methoxide ligands were oriented so as to maintain the optimized C_s symmetry. The C–H distances in the methyl group were set at 1.0 Å.

The results of the SCF–Xα–SW calculation for **2** are summarized in Table 2. There are a number of differences between the molecular orbitals calculated for **2** and those calculated for **1**. Assignment of the nature of the molecular orbitals comes from comparison to Table 1 and from observing the contour maps. The HOMO for **2** (9a″) is still predominantly a Mo–C π-bonding orbital. The 8a″ level is the next lowest in energy. It is centered on the N 2p, O 2p, and $C_{alkoxide}$ 2p atomic orbitals and is significantly

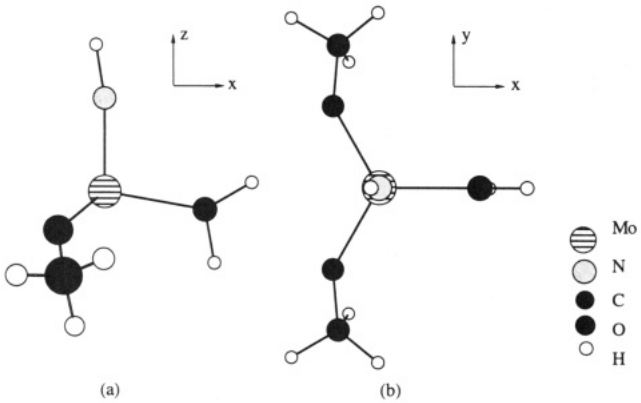

Figure 3. Representation of the $Mo(NH)(CH_2)(OMe)_2$ (**2**), used as a model in SCF–Xα–SW calculations in (a) the xz plane and (b) the xy plane.

higher in energy than the corresponding level (4a″) in **1**. Level 7a″ in **2** is Mo–N π-bonding in the yz plane and is similar to the 5a″ orbital in **1**, while the other Mo–N π-bonding combination, parallel to the N–Mo–C plane, is the 13a′ orbital. The LUMO (14a′), which is qualitatively the same as the 11a′ level in **1** (COO or NOO face attack), is a Mo–N π-antibonding orbital that is metal-centered (34%). The next virtual level, the 15a′ orbital, is also Mo–N π-antibonding and corresponds to the 12a′ level in **1**, while the Mo–C π-antibonding orbital in **2** (10a″) corresponds to the 7a″ orbital in **1**. The similarity of the 14a′ and 15a′ orbitals may be a manifestation of a limitation of the scattered-wave method.[24] Other than the drastic changes in energy observed for the 15a′ orbital in **2** (12a′ in **1**) and the 8a″ orbital in **2** (4a″ in **1**), the electronic structures of the two models are roughly the same. Attempts to determine the electronic structure of a complex containing electron-withdrawing alkoxide ligands, $Mo(NH)(CH_2)(OCF_3)_2$, were complicated by the large number of valence levels and the low symmetry of these model complexes. It is reasonable to propose that strong electron-withdrawing alkoxides might alter the relative energies of the orbitals that determine face selectivity.

The Consequence of Imido and Methylene Bending and Methylene Rotation. The consequence of varying the Mo–N–H angle in **1** from the equilibrium value of 171°, holding all other bond lengths, angles, and atomic parameters constant, is shown graphically in Figure 4. (The numerical values at various angles can be found in Tables S5 and S6 in the supplementary material.) The energies of the molecular orbitals that have considerable contributions from the nitrogen atom, such as the 5a″ and 10a′ levels, change significantly. The Mo–N π-antibonding orbital energy (11a′) is also very sensitive to the Mo–N–H angle. The total energy of the model complex increases as the Mo–N–H angle deviates from the equilibrium value by about 0.2 eV (~5 kcal mol^{-1}), as shown in Figure 5. The value of 171° is found near the minimum of the total energy curve (Figure 5), although the change in total energy upon deviating from this minimum value by 10° is small. The equilibrium value of 171° most likely is the result of perturbation of Mo d orbital combinations by σ- and π-bonding interactions with the other ligands.

The Mo–C–H_{anti} and Mo–C–H_{syn} angles were varied simultaneously, while all other angles, including the H_{anti}–C–H_{syn} angle, were held constant. Molecular orbital energies calculated at each point can be found in Table S8 in the supplementary material. Although energies of

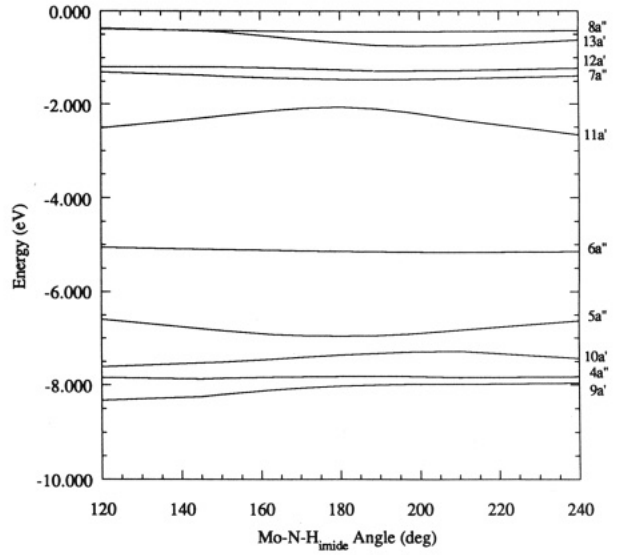

Figure 4. Walsh diagram depicting the change in energy of valence levels 8a″, 13a′, 12a′, 7a″, 11a′ (LUMO), 6a″ (HOMO), 5a″, 10a′, 4a″, and 9a′ as the Mo–N–H angle in **1** (the proton at 120° is oriented anti to the alkylidene ligand) is varied in the Mo-N-H plane of symmetry.

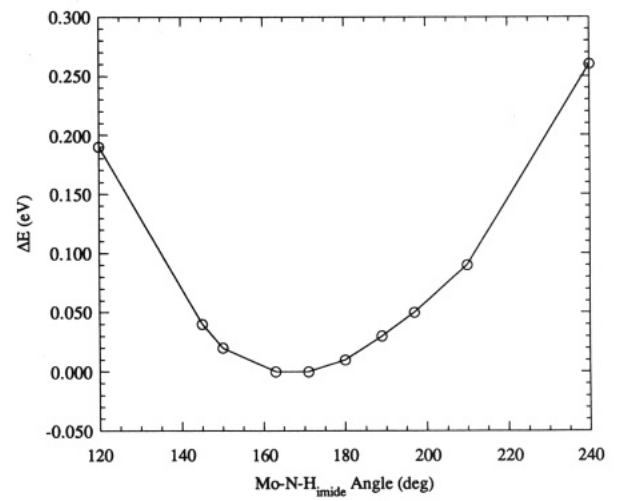

Figure 5. Graphical representation of the change in the calculated total energy of **1** as the Mo–N–H angle is varied from the observed Mo–N–R angle of 171° (where R is oriented anti to the alkylidene).

individual orbitals (Figure 6) change little as Mo–C–H_{anti} is varied from 90° to 140°, there is a shallow minimum for the total energy at a Mo–C–H_{anti} angle of approximately 115° (Figure 7). If the H–C–H angle is held at 110°, then the resulting Mo–C–H_{syn} angle would be 135°. Values observed in X-ray studies of syn rotamers of monosubstituted alkylidene ligands are 140° or greater, although the syn substituent in these cases is considerably more sterically demanding than a proton and therefore could open the Mo–C–R_{syn} angle further for steric reasons. An examination of the energies of orbitals other than those shown in Figure 6 revealed that the energy of the 5a′ orbital, which contains contributions from virtually all atoms in **1**, is particularly sensitive to the Mo–C–H_{anti} angle. As the Mo–C–H_{anti} angle decreases from 120° to 90°, the energy of the 5a′ orbital drops significantly (by ~0.1 eV), while the contributions to the 5a′ molecular orbital from C and H_{anti} (i.e. the C–H bond) increase, as shown in Figure 8. The total energy of the complex rises near 90° (Figure 7) as a result of destabilization of higher energy levels that

Table 2. Energy, Occupancy, and Charge Distribution of the Valence Molecular Orbitals of 2[a]

			charge distribution (%)[b]												
level	energy (eV)	occup[c]	Mo	N	H_{imide}	C	H_{syn}	H_{anti}	O	$C_{alkoxide}$	H1	H2	H3	inter-sphere	outer-sphere	Mo basis functions
11a″	−0.795	0	4	0	0	3	0	0	1	0	0	0	0	55	36	
10a″	−1.089	0	40	6	0	10	0	0	3	1	0	0	0	32	7	d (100)
15a′	−1.530	0	21	3	0	0	0	0	4	0	0	0	0	51	20	p (1) d (100)
14a′	−1.676	0	34	6	0	0	0	0	6	0	0	0	0	41	12	p (1) d (99)
9a″	−4.705	2	29	1	0	31	0	0	7	2	0	0	0	30	0	p (6) d (94)
8a″	−5.856	2	0	8	0	0	0	0	66	4	3	4	0	14	0	
7a″	−6.053	2	3	22	0	0	0	0	46	5	0	2	6	15	0	
13a′	−6.238	2	4	10	0	2	0	0	56	4	2	0	5	14	0	
12a′	−6.891	2	10	8	0	6	0	0	42	7	1	6	3	16	0	s (21) p (25) d (54)
11a′	−7.905	2	23	40	0	1	1	1	12	2	2	1	0	18	0	s (1) p (5) d (94)
6a″	−8.392	2	26	31	0	0	0	0	17	4	2	0	4	16	0	p (1) d (99)
10a′	−9.262	2	38	1	0	39	1	4	2	7	0	2	5	0	0	s (8) p (10) d (82)
9a′	−10.202	2	9	1	0	4	0	0	39	25	1	1	14	4	1	
5a″	−10.297	2	5	0	0	0	0	0	29	33	2	4	22	3	1	
8a′	−11.782	2	8	1	0	0	0	0	32	32	2	22	1	0	0	
4a″	−11.869	2	8	0	0	0	0	0	27	35	7	22	0	0	0	
7a′	−12.401	2	2	0	0	0	0	0	13	40	29	1	13	0	0	
3a″	−12.548	2	8	0	0	0	0	0	21	35	25	0	11	0	0	
6a′	−13.918	2	4	0	0	53	24	19	0	0	0	0	0	0	0	
5a′	−15.664	2	35	51	12	0	0	0	0	0	0	0	0	0	0	s (10) p (20) d (70)
4a′	−17.673	2	4	0	0	0	0	0	21	40	11	16	7	0	1	
2a″	−17.755	2	5	0	0	0	0	0	22	39	11	16	7	0	1	
3a′	−19.886	2	2	0	0	60	17	21	0	0	0	0	0	0	0	
2a′	−22.474	2	5	71	24	0	0	0	0	0	0	0	0	0	0	
1a″	−24.561	2	4	0	0	0	0	0	71	20	2	2	2	0	0	
1a′	−24.582	2	3	0	0	0	0	0	72	20	2	2	2	0	0	

[a] The coordinate system is the same as in Figure 3. Levels above 9a″ are virtual (unoccupied) levels. [b] % of total charge density. [c] Occupancy in electrons.

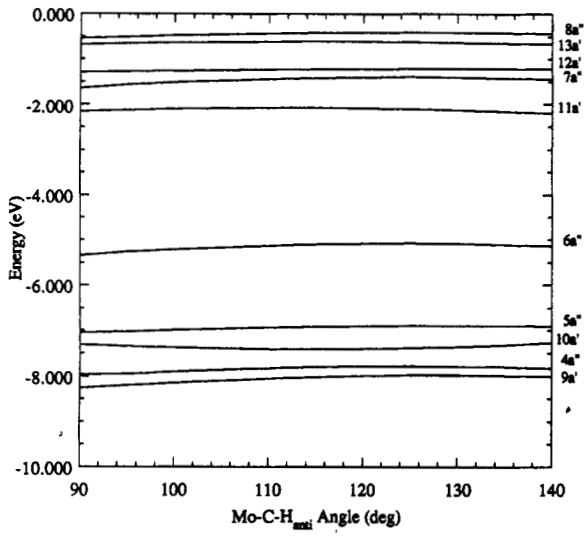

Figure 6. Walsh diagram depicting the change in energy of valence levels 8a″, 13a′, 12a′, 7a″, 11a′ (LUMO), 6a″ (HOMO), 5a″, 10a′, 4a″, and 9a′ as the Mo–C–H_{anti} angle is varied within the plane of symmetry of 1 (Mo–C–H_{anti} = 110° at equilibrium).

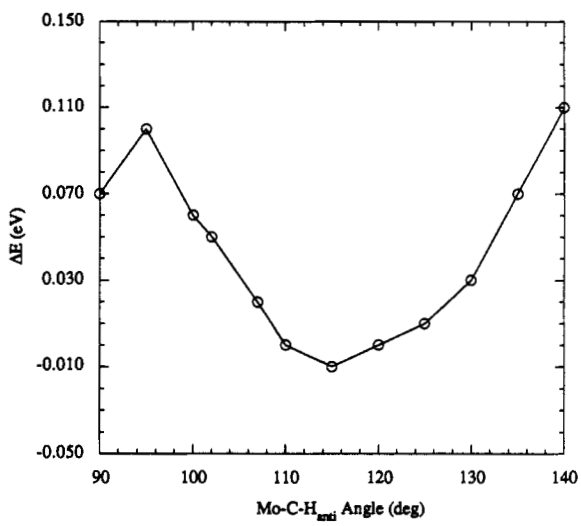

Figure 7. Graphical representation of the change in the calculated total energy of 1 as the Mo–C–H_{anti} angle is varied from the equilibrium value of ~110°.

compete for the same metal-based d-orbitals. The net result is a minimum in total energy at about 115°. The increased contribution of C and H_{anti} orbitals to the 5a′ orbital can be viewed as an agostic interaction,[29] or what was initially called a distortion of an alkylidene toward a "T-shape".[30] The result is a smaller value for J_{CH} between the alkylidene carbon and the anti proton than between the alkylidene carbon and the syn proton. (Note that in a monosubstituted syn alkylidene, the substituent points toward the imido nitrogen atom, contains the H_{anti} proton, and has the smaller value for J_{CHanti}.[9]) The Mo/C–H_{anti} agostic interaction must be weak in these complexes since the Mo–C–H_{anti} angle is not dramatically smaller than the Mo–C–H_{syn} angle, and since J_{CHanti} in a syn rotamer is not dramatically smaller than J_{CHsyn} in an anti rotamer of a monosubstituted alkylidene complex, in general.[31]

It is possible that the minima observed in the alkylidene ligand and imido ligand bending studies are artifacts of the "muffin-tin" potential used in this method.[24] Careful attention to sphere radii using the Norman criterion can help overcome this situation.[25,32] Since in both series of calculations the energies and the virial coefficients do not

(29) Brookhart, M.; Green, M. L. H. *J. Organometal. Chem.* **1983**, *250*, 395.
(30) Schrock, R. R. In *Reactions of Coordinated Ligands*; Braterman, P. R., Ed.; Plenum: New York, 1986.
(31) Feldman, J.; Schrock, R. R. *Prog. Inorg. Chem.* **1991**, *39*, 1.
(32) Takai, Y.; Donovan, M. M.; Johnson, K. H.; Kalonji, G. *Chem. Phys. Lett.* **1989**, *159*, 376.

Table 3. Energy, Occupancy, and Charge Distribution of the Valence Molecular Orbitals of 3[a]

			charge distribution (%)[b]									
level	energy (eV)	occup[c]	Mo	N	H_{imide}	C	$H_{alkylidene}$	O	$H_{hydroxide}$	inter-sphere	outer-sphere	Mo basis functions
8a″	−0.743	0	49	7	0	0	0	9	1	19	16	p (2) d (98)
12a′	−1.242	0	6	0	0	1	0	3	0	49	41	
11a′	−2.015	0	51	2	0	6	0	11	0	24	5	s (1) p (3) d (96)
7a″	−3.433	0	72	5	2	1	2	4	2	14	1	p (1) d (99)
10a′	−4.019	2	12	21	0	30	0	2	0	33	2	p (12) d (88)
6a″	−6.893	2	8	43	0	0	0	27	0	21	1	
9a′	−7.739	2	17	32	0	6	0	20	0	23	1	s (1) p (18) d (82)
8a′	−8.020	2	19	0	0	26	3	38	0	11	1	s (37) p (13) d (50)
5a″	−8.113	2	1	1	0	0	0	79	0	18	0	
7a′	−9.147	2	22	11	0	4	0	43	0	19	0	s (4) p (5) d (92)
4a″	−9.618	2	21	9	0	0	0	51	0	18	0	d (100)
6a′	−9.926	2	31	0	0	13	2	43	0	11	0	s (1) p (1) d (98)
3a″	−13.531	2	3	0	0	46	40	8	2	0	1	
5a′	−13.881	2	15	9	2	0	0	57	15	0	1	s (48) p (11) d (41)
2a″	−14.593	2	18	0	0	6	5	55	14	0	1	p (12) d (88)
4a′	−14.804	2	34	43	11	0	0	9	2	0	1	s (3) p (17) d (80)
3a′	−18.694	2	3	0	0	61	35	0	0	0	1	
2a′	−21.605	2	6	72	21	0	0	0	0	0	0	
1a″	−25.357	2	4	0	0	0	0	82	14	0	0	
1a′	−25.383	2	3	0	0	0	0	83	14	0	0	

[a] Coordinate system is the same as in Figure 1 with the alkylidene ligand rotated 90°. Levels above 10a′ are virtual (unoccupied) levels. [b] % of total charge density. [c] Occupancy in electrons.

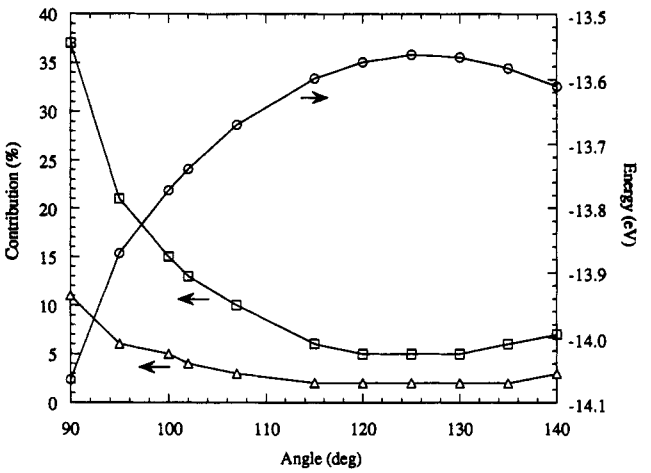

Figure 8. Changes in energy and contributions of C and H_{anti} for the 5a′ orbital during bending of the CH_2 ligand in 1 (—□— represents the contribution of C to the 5a′ orbital, —△— represents the contribution of H_{anti} to the 5a′ orbital, and —○— represents the energy of the 5a′ orbital).

vary symmetrically as the ligands are bent, these results demonstrate a real and not artificial stabilization (see Tables S5 and S7 in supplementary material). Electronic factors influence the orientations of the ligands in the imido alkylidene complexes and optimize orbital stabilization energies at angles other than the ideal 120° in the alkylidene ligand and 180° in the imido ligand.

In order to simplify studies of alkylidene rotation about the Mo–C bond the Mo–C–H_{syn}, the Mo–C–H_{anti}, and the H_{anti}–C–H_{syn} angles were set equal to 120° and the Mo and methylene carbon and hydrogen atoms were constrained to the same plane throughout the rotation process. The N–Mo–C–H_{syn} dihedral angle was then varied from 0° to 90°. Minor changes in bond lengths and angles (i.e. the "flap" angle of the CH_2 group)[16] were not addressed in this study. Calculations in which the methylene ligand was rotated by 10°, 20°, 30°, 40°, 45°, 50°, 60°, 65°, 75°, and 85° were performed in C_1 symmetry (Tables S9 and S10; supplementary material) and calculations at 0° and 90° were performed in C_s symmetry (Table S11; supplementary material). A complete listing of orbital contributions for the "90° rotated model" (3) can be found in Table 3.

Contour plots corresponding to some of the molecular orbitals of 3 are shown in Figure 9. The HOMO, 10a′, is predominantly Mo–C π-bonding and is C-centered (30%) while at the same time it is π-antibonding with respect to the nitrogen (Figure 9a). The antibonding combination of this molecular orbital (11a′) is shown in Figure 9b. Level 9a′ is Mo–N π-bonding, similar to the 10a′ orbital in the ground-state structure. However, there are also strong contributions from the oxygen orbitals to 9a′. The LUMO (7a″; Figure 9c) is essentially a nonbonding metal-centered d_{xy} orbital (72%) which has only minor contributions from each of the other bonding atoms. Finally, the 6a″ orbital shown in Figure 9d depicts the Mo–N π-bonding interaction in the *yz* plane.

The energy levels of 1 (0°) and 3 (90°) are correlated in Figure 10. Pertinent molecular orbitals are shown schematically in order to illustrate how contributions to each level change. Alkylidene ligand rotation leads to competition between the N $2p_x$ and the C $2p_z$ for the Mo d_{xz} atomic orbitals in the 10a′ level (HOMO). Formerly, the 10a′ orbital was the in-plane Mo–N π-bonding orbital. The other major feature of the diagram in Figure 10 is the low lying LUMO (7a″), which is virtually nonbonding, as mentioned above. During the rotation process, the HOMO rises in energy while the LUMO falls in energy, reaching a minimum difference in energy at 90° (Tables S10 and S12 in supplementary material). The weak π-bonding interaction stabilizes the HOMO relative to the LUMO so that the electrons remain spin-paired. The calculations reported here are spin-restricted calculations in which a triplet configuration is not allowed. A calculation in which the spin restriction was removed yielded the same result as for the spin-restricted case.

The change in total energy of the complex as the alkylidene ligand is rotated and all other ligand bond lengths and bond angles are held constant is shown in Figure 11. The total energy increases to a maximum at 90°. The change in energy is ~1.8 eV (~40 kcal mol^{-1}), a difference that is much larger than the largest experi-

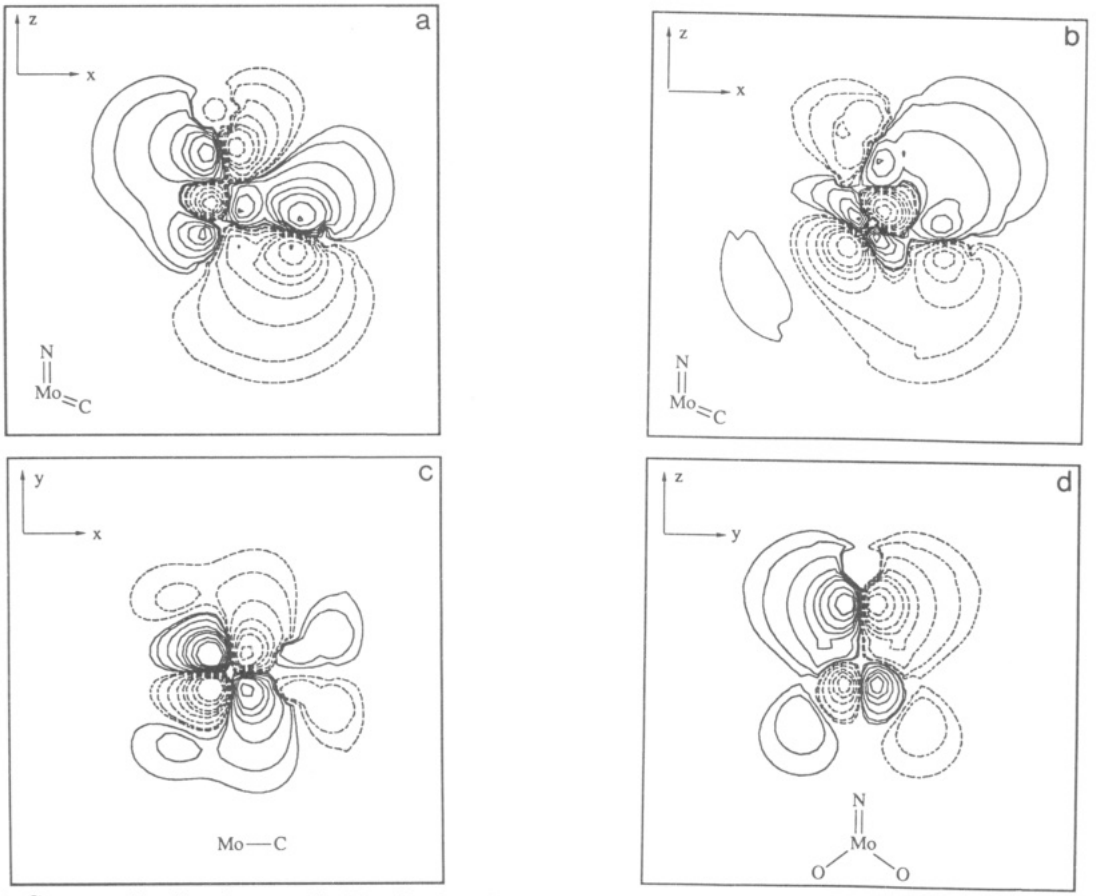

Figure 9. Contour plot showing: (a) the Mo–C π-bonding interaction and Mo–N π-antibonding interaction of the 10a′ orbital (HOMO) in the xz plane; (b) the Mo–C π-antibonding interaction and Mo–N π-antibonding interaction of the 11a′ orbital in the xz plane; (c) the 7a″ orbital (LUMO) in the xy plane; (d) the Mo–N π-bonding interaction of the 6a″ orbital in the yz plane of the rotated alkylidene complex **3**.

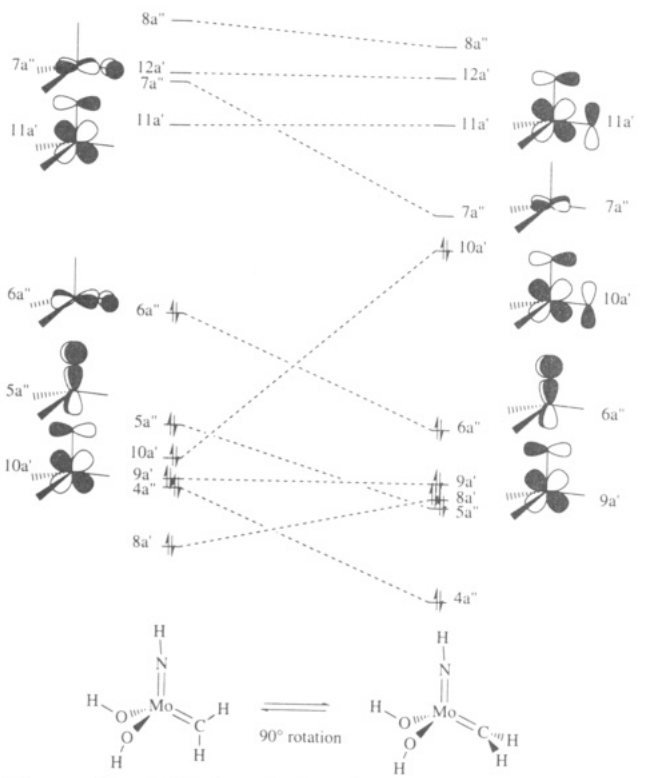

Figure 10. Orbital evolution during alkylidene rotation depicting pertinent π molecular orbitals for **1** (0°) and **3** (90°).

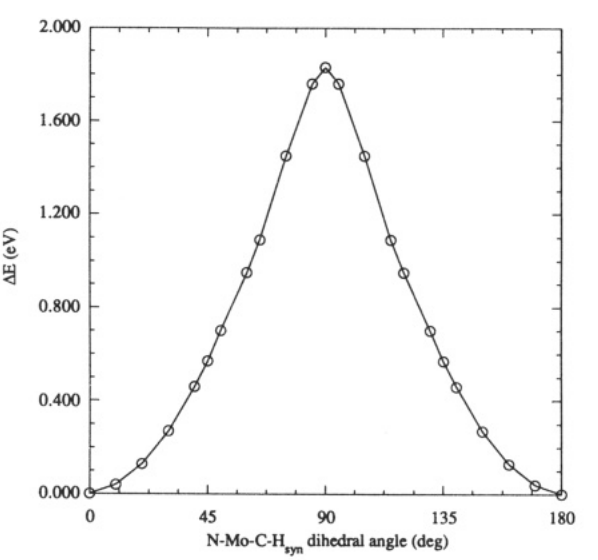

Figure 11. Graphical representation of the change in the calculated total energy of **3** as the N–Mo–C–H_{syn} dihedral angle is varied.

mentally determined barrier to alkylidene rotation in systems of this type (~25 kcal mol^{-1}).[9] Therefore, we varied the Mo–N–H angle, since in previous studies it was found that the imide is likely to bend significantly in a complex containing a rotated alkylidene.[16] The results of varying the Mo–N–H angle in **3**, holding all other parameters constant, are shown in Table S13 (supplementary material). The evolution of selected molecular orbitals as the imide is bent is shown graphically in Figure 12 and a Walsh diagram for this distortion as a function of energy change is depicted in Figure 13. We find that

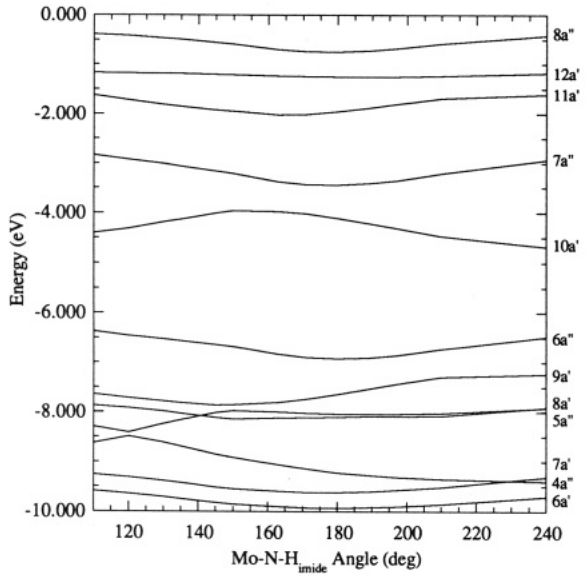

Figure 12. Walsh diagram depicting the change in energy of valence levels 8a″, 12a′, 11a′, 7a″, (LUMO), 10a′ (HOMO), 6a″, 9a′, 5a″, 7a′, 4a″, and 6a′ as the Mo–N–H angle is varied within the plane of symmetry of **3** (the proton at 120° is oriented anti to the alkylidene ligand).

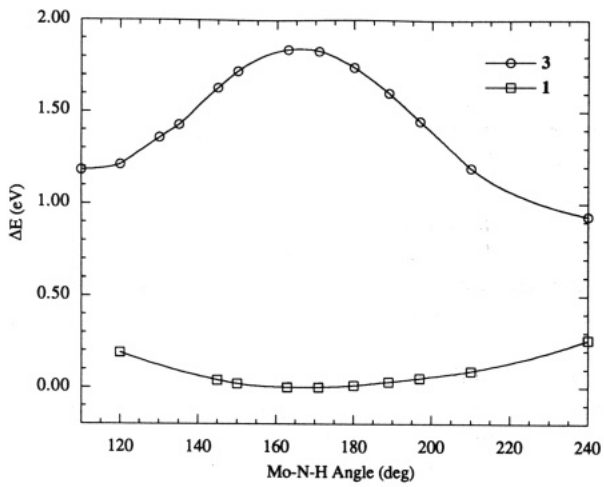

Figure 13. Graphical representation of the change in the calculated total energy of the rotated alkylidene **3** and model **1** as the Mo–N–H angle is varied from the observed Mo-N-R angle of 171° (where R is oriented anti to the alkylidene).

the total energy of the complex containing the rotated methylene ligand decreases substantially when the imido proton is allowed to bend toward or away from the alkylidene carbon, in accord with previous work.[16] The flexible nature of the imido functionality facilitates interconversion of syn and anti rotamers in these complexes. The minimum difference between the total energies of **3** and **1** (at the equilibrium Mo–N–H angle = 171°) shown in Figure 13 (~0.9 eV or ~20 kcal) is found when the imido proton is bent toward the methylene carbon so that the Mo–N–H angle is only 120° (240° in Figure 13), an energy difference that is in excellent agreement with several experimentally determined barriers to rotation in Mo(VI) imido alkylidene complexes of this type.[5,9,33] Since the model cannot take into account steric hindrance, the Mo–N–H angle of 120° should be regarded as the lower limit. Nevertheless, it is clear that **3** will be

(33) Schrock, R. R.; Crowe, W. E.; Bazan, G. C.; DiMare, M.; O'Regan, M. B.; Schofield, M. H. *Organometallics* **1991**, *10*, 1832.

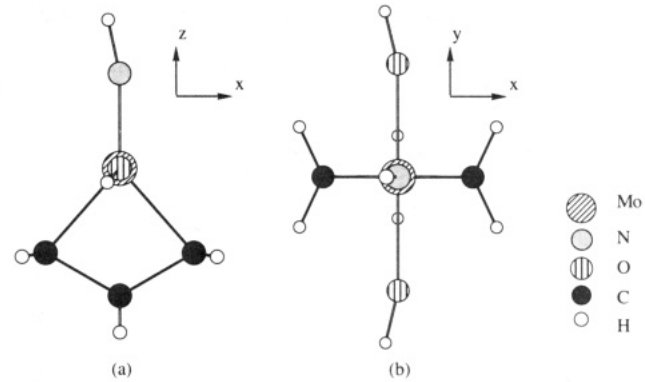

Figure 14. Representation of the Mo(NH)($CH_2CH_2CH_2$)-$(OH)_2$ (**4**) model used in SCF–Xα–SW calculations in (a) the xz plane and (b) the xy plane.

stabilized by imido ligand bending due to diminished competition between the N $2p_x$ and the C $2p_z$ for the Mo d_{xz} atomic orbitals. The alkylidene rotation rate in a 2-*tert*-butylphenyl imido complex increases relative to the 2,6-diisopropylphenyl imido complex,[9] indicating that the bulky group might enhance rotation by encouraging imido ligand bending. The barrier to interconversion of syn and anti rotamers in alkylidene complexes of this type has been found to vary dramatically with the nature of the alkoxide ligand, increasing substantially as the electron-withdrawing ability of the alkoxide increases.[9] The sizable contributions of oxygen orbitals to most of the molecular orbitals in the models studied here are consistent with this observation (Table 1).

Formation of a Metallacycle from a Rotated Alkylidene. In previous theoretical studies of metallacycle formation in Mo(VI) imido alkylidene complexes, the metallacycle was presumed to form via olefin attack on the CNO face of the pseudotetrahedral complex.[14] Indeed there is much evidence in the form of structures of base adducts[31] that the lowest energy structures have the base bound to the CNO face, although it cannot be assumed that the base bonds to the CNO face initially. A metallacycle could form when the olefin attacks the COO face of the complex, if the alkylidene can rotate readily about the Mo–C bond. In this circumstance we would presume that attack by the olefin does not induce rotation of the alkylidene, since addition of bases to these complexes does not induce alkylidene rotation.[9] Nevertheless, concerted alkylidene rotation and metallacycle formation cannot be ruled out. In this section we examine the formation of a metallacyclobutane complex from the complex that contains a "rotated" alkylidene ligand.

The structure used in this set of calculations (**4**; Figure 14) is a pseudotrigonal bipyramid with axial alkoxide ligands and equatorial imido and propanediyl groups. Perhaps the most logical "first metallacycle" that would form when an olefin attacks the COO face of **3** would be the one shown in eq 1. Opening of the O–Mo–O angle and

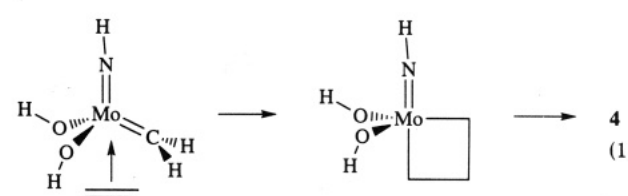

moving the imido nitrogen between the alkoxide oxygens would yield **4**. Only **4** has been examined here because of

Table 4. Energy, Occupancy, and Charge Distribution of the Valence Molecular Orbitals of 4[a]

			charge distribution (%)[b]													
level	energy (eV)	occup[c]	Mo	C_α	$C_{\alpha'}$	C_β	$H_{1\alpha}$	$H_{1\alpha'}$	$H_{1\beta}$	N	H_{imide}	O	$H_{hydroxide}$	inter-sphere	outer-sphere	Mo basis functions
15a′	−3.342	0	43	18	15	2	0	0	1	3	1	2	0	19	0	p (11) d (89)
10a″	−4.257	0	55	0	0	0	0	0	0	27	0	4	0	19	0	d (100)
9a″	−6.029	0	69	0	0	0	0	0	0	0	0	22	0	9	0	d (100)
14a′	−7.042	2	9	10	13	1	0	0	0	44	0	3	0	20	0	
13a′	−7.526	2	43	14	14	2	0	0	1	0	0	5	0	19	0	s (14) p (1) d (85)
8a″	−8.071	2	6	0	0	0	0	0	0	25	0	56	0	14	0	
12a′	−8.737	2	1	0	0	0	0	0	0	1	0	81	0	17	0	
11a′	−9.025	2	6	1	0	0	0	0	0	1	0	76	0	16	0	
7a″	−9.449	2	20	0	0	0	0	0	0	0	0	62	0	17	0	p (1) d (99)
10a′	−10.328	2	26	14	11	15	0	0	0	19	0	0	0	15	0	d (100)
6a″	−10.371	2	32	0	0	0	0	0	0	25	0	26	0	16	0	d (100)
9a′	−11.848	2	21	16	23	19	3	4	0	6	0	0	0	8	0	p (1) d (99)
8a′	−13.248	2	7	22	13	34	3	2	7	6	1	0	0	4	0	
5a″	−14.387	2	1	2	1	38	3	2	39	0	0	11	3	0	0	
4a″	−14.436	2	4	0	0	7	0	0	7	0	0	65	16	0	0	
7a′	−16.023	2	15	0	0	0	0	0	0	2	1	66	17	0	0	s (25) p (2) d (73)
6a′	−18.917	2	35	1	1	1	1	0	0	47	11	2	0	0	0	s (10) p (16) d (75)
3a″	−19.479	2	0	45	8	1	38	8	0	0	0	0	0	0	0	
2a″	−19.952	2	0	9	38	2	8	40	2	0	0	0	0	0	0	
5a′	−21.850	2	0	23	9	24	14	7	22	0	0	0	0	0	0	
4a′	−23.540	2	1	29	30	3	16	21	1	0	0	0	0	0	0	
3a′	−24.851	2	2	4	5	9	2	3	6	50	19	0	0	0	0	
2a′	−25.233	2	3	11	12	21	5	6	12	23	7	0	0	0	0	
1a″	−26.773	2	1	0	0	0	0	0	0	0	0	82	17	0	0	
1a′	−26.965	2	1	0	0	0	0	0	0	0	0	83	16	0	0	

[a] Coordinate system is the same as in Figure 14. Levels above 14a′ are virtual (unoccupied) levels. [b] % of total charge density. [c] Occupancy in electrons.

its relatively high symmetry, and we can assume that 4 is formed more or less directly in a concerted process. (The fact that no metallacyclobutane complexes have been observed that have a structure corresponding to that of 4 is not necessarily a negative feature of this model, since it is an intermediate in the metathesis process.) The bond lengths and bond angles for the metallacycle and the axial alkoxides are adapted from crystallographically characterized trigonal bipyramidal tungstacyclobutane complexes.[34,35] The imido ligand bond length and the Mo–N–H bond angle was taken from a five-coordinate Mo(VI) imido alkylidene complex.[33] As in the other models, the simple proton derivatives of the ligand were used and minor structural modifications were made in order to maintain C_s symmetry for the complex. A list of bond lengths, bond angles, dihedral angles and atomic coordinates used in this model can be found in the supplementary material (Tables S15 and S16). A summary of the molecular orbital information obtained from the SCF–Xα–SW calculation is listed in Table 4.

Contour plots for selected molecular orbitals are shown in Figure 15. The virtual 15a′ orbital (Figure 15a) illustrates Mo–C σ-antibonding interactions. The Mo–N and Mo–O π-antibonding interactions of the 10a″ level are shown in Figure 15b. The LUMO in this hypothetical metallacycle is the 9a″ orbital, which is exclusively Mo–O π-antibonding in character (Figure 15c). The HOMO (13a′; Figure 15d) is a metal–carbon σ-bonding molecular orbital. The HOMO and LUMO are separated by nearly 1 eV. The 13a′ level is also a metal–carbon σ-bonding level with some C–C bonding interactions (Figure 15e). The 8a″ orbital (Figure 15f) is predominantly a π-bonding Mo–N interaction in the *yz* plane. The Mo–N π-bond is mixed with other metallacycle σ-bonding combinations in the 10a′ orbital (Figure 15g) and the 9a′ orbital (Figure 15h). The 8a′ orbital is predominantly C–C σ-bonding (Figure 15i). The σ-bonding and σ-antibonding molecular orbitals of the metallacycle are similar to those described recently by Folga and Ziegler in a metallacyclobutane complex with a different overall structure.[14] An orbital interaction diagram (Figure 16) shows the evolution of the metallacycle molecular orbitals from the molecular orbitals of the rotated alkylidene complex and ethylene. The major metal–carbon σ-bonding interactions are derived from Mo–C π-bonding and π-antibonding orbitals as well as C–C π-bonding and π-antibonding orbitals. On the basis of these results we must consider the possibility in future work that a metallacyclobutane complex could form when an olefin attacks the COO face of the pseudotetrahedral catalyst in which the alkylidene is rotated by 90°, in addition to previously discussed mechanisms.[14]

Discussion

The results of SCF–Xα–SW calculations reported here are consistent with reactivity patterns of these complexes. In the basic model (1) the HOMO is the M–C π-bond. The contributions by the C 2p and the Mo 4d atomic orbitals are approximately equal, i.e., the Mo=C bond is relatively nonpolar, a fact that may help explain why Mo complexes are relatively tolerant of functionalities such as esters and nitriles compared to W or (especially) Ta complexes. The alkoxide oxygen 2p orbitals contribute to a significant extent to most molecular orbitals, which complicates a detailed analysis of the electronic structure of these molecules, but at the same time helps explain the long-standing conclusion on the basis of experimental work carried out over the past five years that the reactivity of

(34) Feldman, J.; DePue, R. T.; Schaverien, C. J.; Davis, W. M.; Schrock, R. R. In *Advances in Metal Carbene Chemistry*; Schubert, U. Ed.; Kluwer: Boston, 1989; p 323.
(35) Feldman, J.; Davis, W. M.; Schrock, R. R. *Organometallics* **1989**, *8*, 2266.

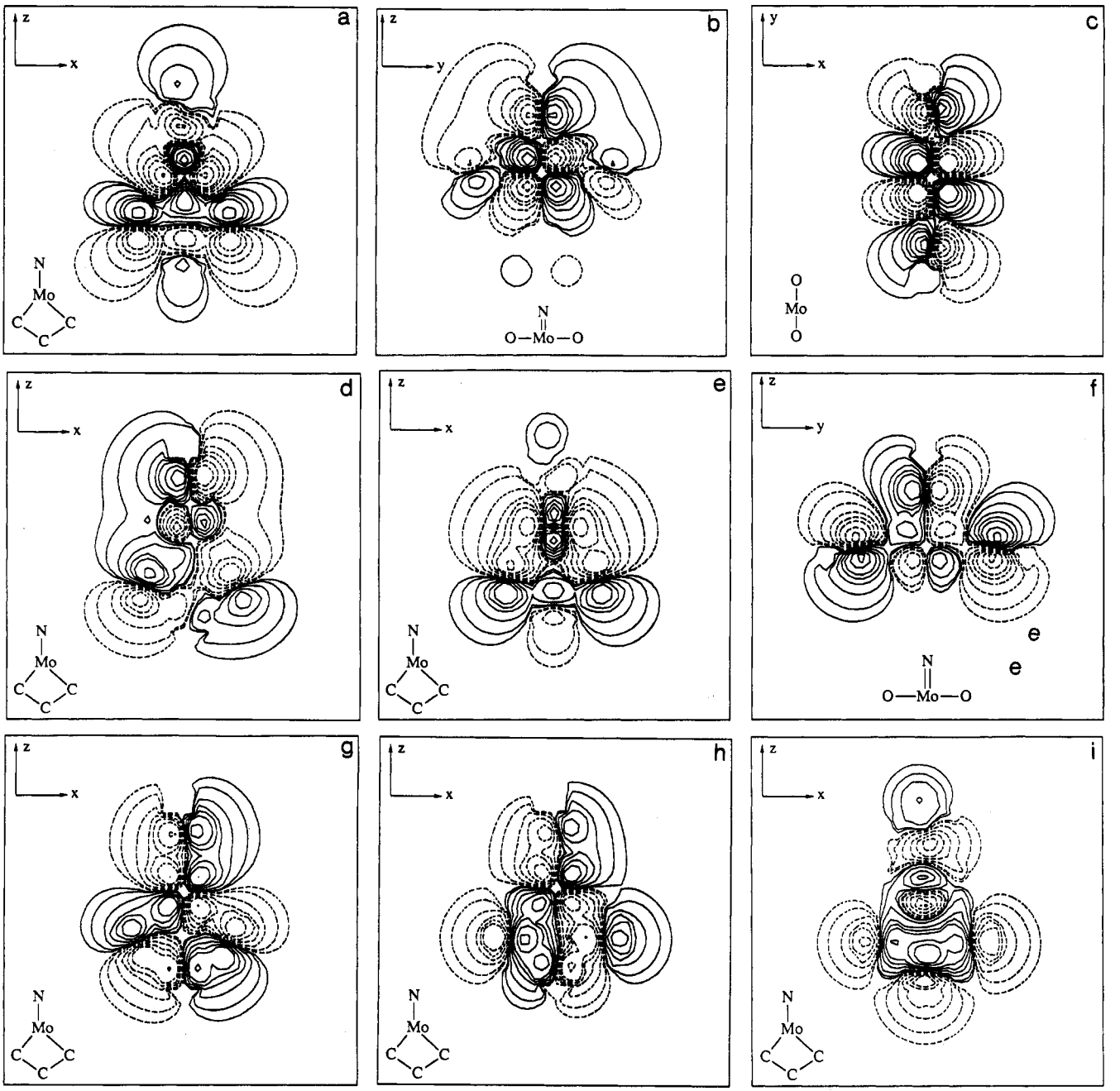

Figure 15. Contour plot showing: (a) the Mo–C σ-antibonding interaction of the 15a′ orbital in the xz plane; (b) the Mo–N π-antibonding interaction of the 10a″ orbital in the yz plane; (c) the Mo–O π-antibonding interactions of the 9a″ orbital in the xy plane; (d) the Mo–C σ-bonding interactions of the 14a′ orbital in the xz plane; (e) the Mo–C σ-bonding interactions of the 13a′ orbital in the xz plane; (f) the Mo–N π-bonding interactions of the 8a″ orbital in the yz plane; (g) the Mo–C and C–C σ-bondng interactions of the 10a′ orbital in the xz plane; (h) the Mo–C and C–C σ-bonding interactions of the 9a′ orbital in the xz plane; (i) the Mo–C and C–C σ-bonding interactions of the 8a′ orbital in the xz plane.

the catalyst is extremely sensitive to the electronic nature of the alkoxide ligand.[2,6,7,9-11,27,33,34,36]

The LUMO in both **1** and **2** is the M–N π-antibonding orbital in the alkylidene plane, which is largely metal-centered on the COO face of the pseudotetrahedral complex, trans to the imido ligand. Five-coordinate adducts in which the base has added to this face intramolecularly have been observed,[7,37] but five-coordinate adducts formed from external bases are more frequently observed in which the base apparently has added to the CNO face of the pseudotetrahedral complex.[33] Although direct attack of a base on the CNO face would appear to require attack on a higher energy virtual orbital than COO attack, CNO attack is sterically perhaps more favorable, and must still be considered. Another possibility is that the base binds to the COO face and the five-coordinate complex then undergoes a series of Berry-type pseudorotations in order to minimize competition between the π-bonding ligands. It is clear at this stage that syn and anti rotamers of monosubstituted alkylidene complexes can have dramatically different reactivities and that changes in the steric and electronic nature of the imido ligand (e.g., 2,6-disubstituted phenylimido to adamantylimido[9]) can have major consequences; in each case a

(36) Schrock, R. R.; DePue, R.; Feldman, J.; Schaverien, C. J.; Dewan, J. C.; Liu, A. H. *J. Am. Chem. Soc.* **1988**, *110*, 1423.
(37) Johnson, L. K.; Virgil, S. C.; Grubbs, R. H.; Ziller, J. W. *J. Am. Chem. Soc.* **1990**, *112*, 5384.

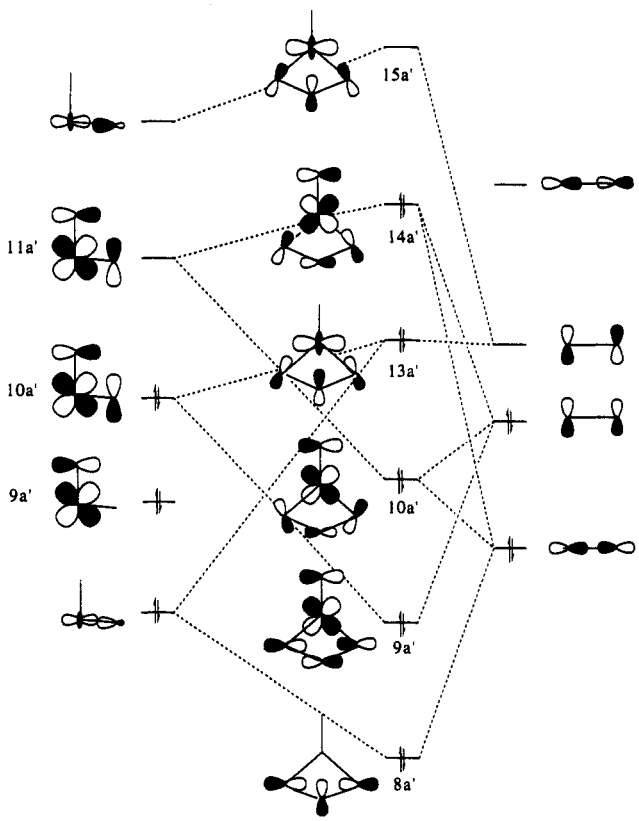

Figure 16. Orbital interaction diagram for the formation of a metallacyclobutane on the COO face of a rotated pseudo-tetrahedral alkylidene complex (3).

"switch-over" from COO to CNO face attack (or vice versa) could possibly be involved. Finally, we have to consider the possibility that many observed base adducts or metallacycles are thermodynamic products that might be the end result of some rearrangement process, a circumstance that is today viewed as the more likely in homogeneous catalysis systems.[38]

Studies involving methylene or imido ligand bending have indicated that there are electronic reasons for deviations from ideality in the structures of the imido alkylidene complexes and that a weakly stabilizing agostic interaction is present in these terminal alkylidene complexes that is similar to the strong agostic interaction described some time ago in Ta(V) alkylidene complexes.[30] The abundance of strong π-donor ligands monopolizes the available metal d orbitals, rendering the magnitude of this agostic interaction weak in the complexes described here. Bending of the imido ligand is an important stabilizing feature in a "rotated" alkylidene complex, lowering the activation energy by approximately 50%. (Cundari and Gordon also found that the imido ligand bends toward the alkylidene ligand in the *xz* plane, minimizing competition for the d_{xz} orbital and allowing a stronger Mo–C π-bond to be formed.[16]) Experimental evidence suggests that the rate of alkylidene ligand rotation is enhanced by approximately 3 orders of magnitude in *ortho*-substituted phenylimido complexes such as Mo(N-2-*t*-BuC_6H_3)(CHCMe$_3$)[OCMe(CF$_3$)$_2$]$_2$.[9] A single bulky group in the *ortho* position most likely promotes bending of the imide which consequently lowers the barrier to alkylidene rotation.

(38) Halpern, J. *Science* **1982**, *217*, 401.

Alkylidene rotation is clearly an important factor in determining both the rate and the stereochemistry of reactions between the alkylidene and olefins.[5,9] Metallacycle formation by olefin attack on the COO face in a species in which the alkylidene is at least partially rotated has some appeal when alkylidene rotation is known to be rapid relative to the rate of reaction with substrate.[9] Although the lifetime of the fully rotated alkylidene species is likely to be relatively short, the "rotated" alkylidene complex would be expected to be much more reactive, even if one considers only spin-paired descriptions in the rotated alkylidene complex. The rate of rotation has been found to vary dramatically with the electronic character of the alkoxide ligands.[5,9] But the rate of alkylidene ligand rotation and the stability of the rotated alkylidene also should vary with the steric and electronic nature of the imido ligand. Preliminary studies of alkylidene rotation in complexes that contain different imido ligands suggests that this is the case,[5,9] and that alkylidene ligand rotation may be an important phenomenon in a variety of classical as well as nonclassical (well-characterized) olefin metathesis catalysts.

Experimental Section

SCF–Xα–SW calculations[23,24] were carried out on a Sun SPARCstation 2. Atomic coordinates were calculated for the models in idealized geometries as outlined below. Atomic radii were scaled uniformly using the Norman criterion[39] until the calculation satisfied the virial theorem ($-2T/V = 1.00000$ in most cases). Appropriate atomic α values (exchange correlation parameters) were taken from the literature.[25,40-42] Molecular α values were calculated as the weighted average of the atomic α values, based on the number of valence electrons for each atom. The calculations were converged to self-consistency (less than 0.01% change). Contours are drawn for charge-densities ±0.4, ±0.2, ±0.15, ±0.1, ±0.075, ±0.05, ±0.025, ±0.01, and ±0.005 (e/bohr^3)$^{1/2}$ in all contour maps.

Mo(NH)(CH$_2$)(OH)$_2$ (1). The calculation for 1 was carried out in C_s symmetry using the atomic coordinates, radii and α values listed in Table S2 in the supplementary material. Bond lengths and angles that were employed can be found in Table S1 in the supplementary material. The calculation converged with a virial ratio ($-2T/V$) of 1.000002, and E_{total} = −114902.04 eV.

Mo(NH)(CH$_2$)(OMe)$_2$ (2). The calculation for 2 was carried out in C_s symmetry using the atomic coordinates, radii, and α values listed in Table S4 in the supplementary material. Bond lengths and angles that were employed can be found in Table S3 in the supplementary material. The calculation converged with a virial ratio ($-2T/V$) of 0.999982, and E_{total} = −117075.11 eV.

Mo–N–H Bending. Complex 1 was used as the basis for these calculations. The Mo–N–H angle was varied from the core structural angle of 171° (dihedral angle of H–N–Mo–C = 180°). At each angle listed in Table S5 in the supplementary material, a complete SCF–Xα–SW calculation was performed. The results of the calculations are summarized in Table S5, and the molecular orbital energies are listed in Table S6 in the supplementary material.

Mo–C–H$_{anti}$ Bending. Complex 1 was used as the basis for the calculations. The Mo–C–H$_{anti}$ angle was varied from the core structural angle of 110° (H$_{anti}$–C–H$_{syn}$ = 110°). At each angle listed in Table S6 in the supplementary material, a complete SCF–Xα–SW calculation was performed. The results of the calculations are summarized in Table S7 in the supplementary material and the molecular orbital energies are listed in Table S8 in the supplementary material.

(39) Norman, J. G., Jr. *Mol. Phys.* **1976**, *31*, 1191.
(40) Schwarz, K. *Phys. Rev. B* **1972**, *5*, 2466.
(41) Schwarz, K. *Theor. Chim. Acta* **1974**, *34*, 225.
(42) Slater, J. C. *Int. J. Quantum Chem.* **1973**, *S7*, 533.

$Mo–CH_2$ Rotation. Complex 1 was used as the basis for these calculations. The N–Mo–C–H_{syn} dihedral angle was varied from 0° (Mo–C–H_{anti} = Mo–C–H_{syn} = H_{anti}–C–H_{syn} = 120° throughout this set of calculations). The points at 0° and at 90° were calculated in C_s symmetry while the other points were calculated in C_1 symmetry. At each angle listed in Table S9 in the supplementary material, a complete SCF–Xα–SW calculation was performed. Atomic coordinates, radii, and α values for the rotated alkylidene complex 3 are listed in Table S11 in the supplementary material. The results of the calculations are summarized in Table S9 and the molecular orbital energies are listed in Tables S10 and S12 in the supplementary material. The data points from 90° to 180° were generated by symmetry.

The Mo–N–H angle was varied from the core structural angle of 171° (dihedral angle of H–N–Mo–C = 180°) in 3. At each angle listed in Table S13 in the supplementary material, a complete SCF–Xα–SW calculation was performed. The results of the calculations are summarized in Table S13 in the supplementary material and the molecular orbital energies are listed in Table S14.

$Mo(NH)(CH_2CH_2CH_2)(OH)_2$ (4). The calculation for 4 was carried out in C_s symmetry using the atomic coordinates, radii, and α values listed in Table S16 in the supplementary material. The structural characteristics of the model are listed in Table S15 in the supplementary material. The calculation converged with a virial ratio ($-2T/V$) of 1.000349, and E_{total} = −117041.04 eV.

Acknowledgment. We thank the National Science Foundation (CHE 91 22827) for supporting this work.

Supplementary Material Available: Table S1. List of bond lengths, angles, and dihedral angles in 1. Table S2. Atomic positional coordinates, radii, and α values used for 1. Table S3. List of bond lengths, angles, and dihedral angles in 2. Table S4. Atomic positional coordinates, radii, and α values used for 2. Table S5. Total energy and $-2T/V$ values obtained during Mo–N–H angle variation in 1. Table S7. Total energy and $-2T/V$ values obtained during Mo–C–H_{anti} angle variation in 1. Table S9. Total energy and $-2T/V$ values obtained during Mo–CH_2 rotation in 1. Table S11. Atomic positional coordinates, radii, and α values used for 3. Table S13. Total energy and $-2T/V$ values obtained during Mo–N–H angle variation in 3. Table S15. List of bond lengths, angles, and dihedral angles in 4. Table S16. Atomic positional coordinates, radii, and α values used for 4 (in bohr). Table S6. Energies of the valence orbitals in 1 as the Mo–N–H angle is varied. Table S8. Energies of the valence molecular orbitals in 1 as the Mo–C–H_{anti} angle is varied. Table S10. Energies of the valence orbitals for 1 as the CH_2 ligand is rotated out of the N–Mo–C plane. Table S12. Energies of the valence orbitals of 1 and 3. Table S14. Energies of the valence orbitals in 3 as the Mo–N–H angle is bent (16 pages). Ordering information is given on any current masthead page.

OM940063O